Science of Sintering, **55** (2023) 539-547

https://doi.org/10.2298/SOS220809022M

UDK: 661.112.3; 53.086

The Crystal Growth of NASICON Phase from the Lithium Germanium Phosphate Glass

Srđan D. Matijašević[1*)], Vladimir S. Topalović[1], Veljko V. Savić[1], Nebojša J. Labus[3], Jelena D. Nikolić[1], Snežana N. Zildžović[1], Snežana R. Grujić[2]

[1]Institute for Technology of Nuclear and Other Mineral Raw Materials (ITNMS), 86 Franchet d Esperey St., 11000 Belgrade, Serbia

[2]Faculty of Technology and Metallurgy, University of Belgrade, 4 Karnegijeva St.,11000 Belgrade, Serbia

[3]Institute of Technical Sciences of SASA, Knez-Mihailova 35/IV, 11000 Belgrade, Serbia

Abstract:

The crystal growth rate of $LiGe_2(PO_4)_3$ phase from lithium germanium-phosphate glass was studied. The glass have been homogenized using the previously established temperature-time conditions, which make it possible to remove volatile substances from the glass melt. The atomic absorption spectrophotometry (AAS) was used to determine the chemical content of the obtained glass and scanning electron microscope (SEM) were used to reveal the isothermal process of crystal growth. The crystal growth rates were determined experimentally and theoretically.

***Keywords**: Lithium germanium-phosphate glass; Crystal growth; SEM.*

1. Introduction

Glass is a solid, isotropic substance with a complex structure. It is formed by continuous cooling of the melt until its viscosity becomes high enough to solidify in the glassy state.

In the area of low temperatures, the behavior of glass corresponds to the behavior of elastic solids. At high temperatures, the glass acts as an ideal liquid substance. Many properties of glass makes it suitable for use, transparency, chemical inertness, durability, strength and others [1-3].

Thanks to a number of specific properties that germanate glasses can have, their application as a material in various technological fields can be very wide: electronics and optoelectronics for sensors, insulating and hermetic connections, ionic conductors, batteries, optical fibers, IR optics, etc. [4-7]. Phosphate glasses due to the properties of bioactivity and biocompatibility of phosphorus are used in medicine as bone and dental implants [8-9]. The studies of crystallization of Li_2O-Al_2O_3-GeO_2-P_2O_5 glasses showed that one of dominant crystal phase precipitated in glass matrix is NASICON-type $LiGe_2(PO_4)_3$ crystals [10].

The phenomenon of crystallization (melting) is key to understanding and controlling the formation of glass. The crystallization process is controlled by two parameters - the rate of nucleus formation and the rate of crystal growth, which depend on the temperature in different ways. The rates of these processes determine the crystalline product quality [11]. In

*) **Corresponding author:** s.matijasevic@itnms.ac.rs

order to achieve enhanced control over the crystal nucleation and growth in a continuous crystallization processes, a higher level of nucleation understanding and control is needed. Crystal growth is controlled either by processes at the formed phase boundary or by diffusion in the melt. In the process of crystallization, stable nuclei continue to grow. Crystallization is called polymorphic if the crystals growing are of the same composition as the melt. In case the compositions of the melt and the crystals are different, the crystallization is marked as primary. Generally speaking, in polymorphic crystallization, the growth rate is controlled by reactions at the interface, in contrast to primary crystallization, where the diffusion rate is determining step.

The focus of the presented research is the determinations of the crystal growth rate in Li_2O-Al_2O_3-GeO_2-P_2O_5 undercooled melt.

2. Materials and Experimental Procedures

The glass was prepared by melt quenching procedure of reagent-grade (99.99%) Li_2CO_3, Al_2O_3, GeO_2, and $(NH_4)_2HPO_4$ in a covered platinum crucible. The components were thoroughly mixed and heated stepwise up to 300°C for 16 h to remove volatile substances. The melting was performed in an electric furnace CARBOLITE BLF 17/3 at T=1400°C during t=0.5 h.

2.1. Chemical analysis

The chemical analysis was performed using spectrophotometer AAS PERKIN ELMER Analyst 300. The method of atomic absorption spectrophotometry (AAS) was used to determine the content of oxides, Li_2O, GeO_2, P_2O_5, Al_2O_3 in glass, after the dissolution of the sample in NaOH, and the composition was determined by analyzing the content of oxide`s cations in the solution. The measurement uncertainty was 0.49%.

2.2. Crystallization of glass under isothermal conditions and determination of growth rates

For isothermal crystallization experiments, compact samples of the glass of suitable dimensions were used, which were heated in an electric furnace CARBOLITE CWF 13/13 with a heating rate regulator and a temperature accuracy of ± 1°C. Samples of glass were placed on platinum plates and heated at a rate of β =10 °Cmin^{-1}. The temperature range of crystallization was previously determined on DTA/DSC [10, 19]. Upon reaching the selected nucleation and crystallization temperature, the samples were isothermally heated for a different time duration from 30 min up to 30 h [12]. After the crystallization was completed, the samples were taken out of the furnace, and then partly prepared in the form of XRD sample powder, and partly in the form of compact pieces of suitable fractures for SEM. The SEM was used to analyze the microstructure of the glass samples and the results were used to determine the crystallization mechanism, crystal growth morphology and crystallization temperature dependence. In order to determine the growth rate U, the crystal diameter dependencies $d(t)$ were constructed for a series of samples held for different growth times (t) at a specified temperature (T). It was revealed that these dependencies exhibit a linear behavior, which allows us to determine the crystal growth rate from their slope [13].

2.3. Scanning electron microscope (SEM)

The surface and fractures (fracture surfaces) of the crystallized samples were analyzed by SEM MIRA3 XMU. The MIRA 3 XMU scanning electron microscope uses a high-brightness Schottky emitter with high contrast and resolution of up to 1.0 nm at 30kV and with a magnification up to 10^6 X. The recording of the sample surface is in stereoscopic 3D mode with the possibility of a high sampling speed of up to 20 ns/pixel. All samples were coated in gold on a Jeol JFC 1100 sputter-coater before analysis. The SEM results were used to determine the crystallization mechanism, crystal growth morphology and kinetics of the isothermal crystallization process.

3. Results and Discussion

The glass mixture for obtaining the selected glass composition was melted in an electric furnace. The resulting melts were poured between two steel plates and cooled in the air. During cooling, the melt solidified into a transparent, homogeneous and colorless glass. The results of the chemical analysis show that a glass composition of $22.5Li_2O{\cdot}10Al_2O_3{\cdot}30GeO_2{\cdot}37.5P_2O_5$ (mol%) (LAGP) was obtained.

Isothermal crystallization experiments were performed on bulk glass samples in order to determine the crystallization mechanism, crystal growth rate and temperature dependence. The crystal growth of the $LiGe_2(PO_4)_3$ phase (JCPDS 80-1922, rhombohedral, space group R3-c (167), polymorphic crystallization, XRD analysis, figure not shown, [10,14-16]) were examined by SEM analysis.

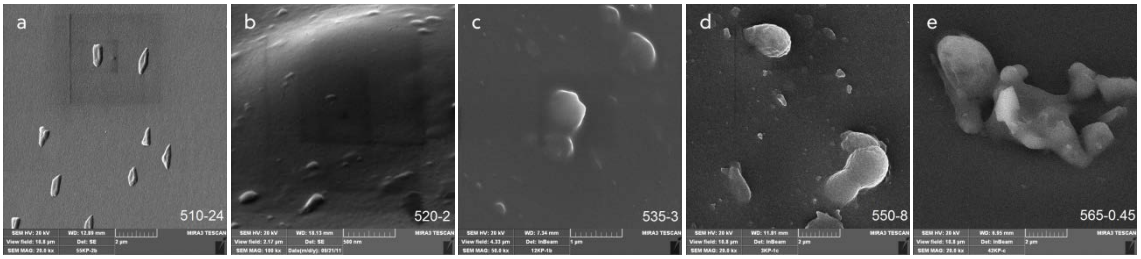

Fig. 1. SEM micrograph of treated LAGP glass at: a) 510°C -24h, b) 520°C -2h, c) 535°C -3h, d) 550°C -8h, e) 565°C -0.45h, respectively.

The results shown in Fig.1, indicate that the nucleation process commenced within the bulk of the melt and that the morphology of the growing crystals was spherical in nature (volume crystallization, [17]). It can be noticed how the size of the crystals increases with increasing temperature and heat treatment time. For the LAGP glass sample, the dependence of the mean crystal diameter (d) on the heat treatment time at the nucleation temperatures (510, 520, 535, 550 and 565°C) is shown in Fig. 2.

Tab. I Crystal growth rates (U), at different temperatures.

Ordinal number	T_n [°C]	U [ms^{-1}]
1	510	$1.54{\cdot}10^{-13}$
2	520	$2.27{\cdot}10^{-12}$
3	535	$5.61{\cdot}10^{-12}$
4	550	$1.42{\cdot}10^{-11}$
5	565	$1.68{\cdot}10^{-11}$

From the slope of the lines (d_{sr}) = f (t), crystal growth rates were determined for each nucleation temperature T_n. Table I, shows the growth rates of LAGP glass crystals at different temperatures determined by the isothermal method used to process the results.

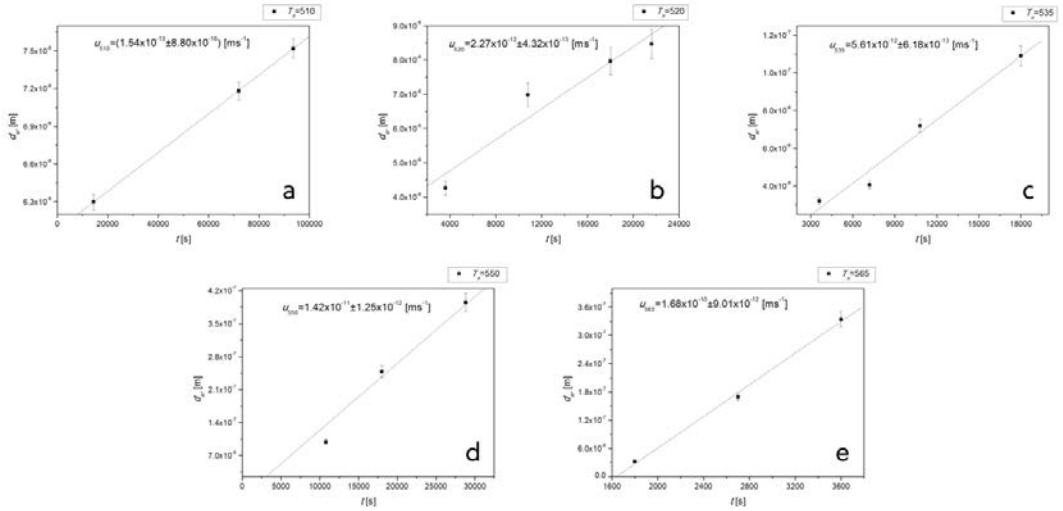

Fig. 2. Dependence of d_{sr} on heat treatment time at crystal nucleation temperatures in LAGP glass at a) T_n = 510 °C, b) T_n = 520 °C, c) T_n = 535 °C, d) T_n = 550 °C, e) T_n = 565 °C, respectively.

The temperature dependence (510-565°C) of the growth rate of the $LiGe_2[PO_4]_3$ (U_{exp}) crystals in LAGP glass is shown in Fig. 3.

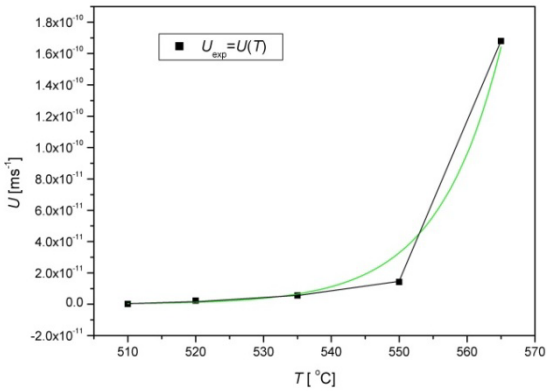

Fig. 3. Diagram of the temperature dependence of experimentally determined growth rate of $LiGe_2[PO_4]_3$ phase crystals in LAGP glass.

In the region shown, the crystal growth rate increases with temperature significantly at T> 550°C (Fig. 3). This indicates the possibility of partial overlap of the nucleation region and crystal growth. A similar conclusion was observed based on DTA analysis [17].

In the general case, the crystal growth rate from the undercooling melts can be represented by the equation [18]:

$$U = f \cdot \lambda \cdot \nu \left[\exp\left(-\frac{\Delta G'_D}{kT} \right) \right] \qquad (1)$$

where: f is the proportion of sites suitable for crystal growth; λ - a distance of atom transport through the crystal/melt boundary (approximately corresponds to the diameter of molecules) v - atomic vibration frequency ($v = kT/h$); $\Delta G'_D$ - free activation energy for transporting atoms across the crystal/melt boundary (kinetic barrier to crystal growth); k is Boltzman constant and T is the temperature in Kelvin.

Tab. II Parameters for calculating the crystallization rate and crystal growth [12, 19].

k=1.380622· 10^{-23} J K^{-1}	A = - 2.8361
$l_{P\text{-}O}$ = 1.8 · 10^{-10} m	B = 3430.60
λ = 20.5696 · 10^{-10} m	T_o = 555.8459 [K]
T_m = 1368.65 K	ΔS_m= 44.08 J mol^{-1} K^{-1}
ΔH_m =60.325 $kJmol^{-1}$	V_m=121.09 ·10^{-6} m^3mol^{-1}

From Table II, the entropy change can be considered as large and the crystal growth process can be described as - growth at the "smooth" boundary by a spiral screw dislocation model [19]. The fraction of the preferred growth sites for the screw dislocation model is expressed by the following relation [20]:

$$f = \frac{\lambda \cdot \Delta H_m \cdot \Delta T}{4 \cdot \pi \cdot \sigma \cdot V_m \cdot T_m} \approx \frac{\Delta T}{2\pi \cdot T_m} = \frac{1 - T_r}{2\pi} \qquad (2)$$

where: T_m is the thermodynamic melting point, $\Delta T = T_m - T$ is undercooling interval, $T_r = T/T_m$ is the reduced temperature, ΔH_m is the molar enthalpy of the melting and ΔV_m the molar volume, σ is the surface energy of the crystal [12, 19].

After several rearrangements and transformations the final form for the crystal growth rate can be written as:

$$U = \left(\frac{1 - T_r}{2\pi}\right)\left(\frac{kT}{l^3 10^A}\right)\lambda \cdot \exp\left(\frac{-2{,}3 \cdot B}{T - T_0}\right)\left\{1 - \exp\left[-\frac{\Delta S_m}{R}\left(\frac{1}{T_r} - 1\right)\right]\right\} \qquad (3)$$

here l is the bond length, A and B are the constants from Vogel - Fulcher - Taman (VFT) Eqs., ΔS_m is melting entropy and R is gas constant. The temperature dependence of the theoretical growth rate of U_{teo} crystals was calculated using Eqs. (3), using the parameters shown in Table II. The dependence of U_{teo} compared with the experimental values of U_{exp} is shown graphically in Fig. 4.

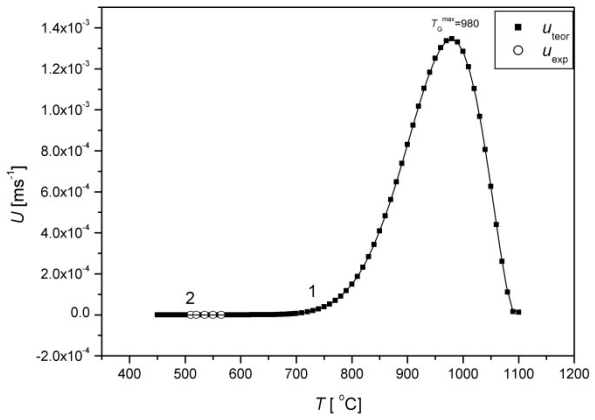

Fig. 4. Theoretical and experimental temperature dependence of U for tested LAGP glass.

Fig. 4, shows that there is a good agreement between the calculated (curve 1) and experimental values (point on line 2), which indicates that the proposed theoretical model (screw dislocation) describes well the crystal growth rate of this glass. It can be noticed that the theoretical temperature of the maximum growth rate of $LiGe_2[PO_4]_3$ phase crystals is T_{Gteo}^{max} = 980°C, and the maximum growth rate is $U_{teo}^{max} = 1.35 \cdot 10^{-3}$ ms^{-1}.

Fig. 5, shows a parallel theoretical and experimental growth rate of $LiGe_2[PO_4]_3$ phase crystals in LAGP glass in the investigated temperature range.

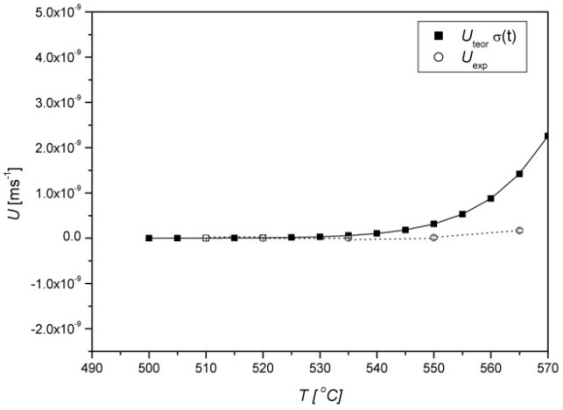

Fig. 5. Comparative presentation of the theoretical and experimental growth rate of crystals in the temperature range 500-570 °C.

It can be noticed (Fig. 5) that between the theoretical (U_{teor}) and experimental values (U_{exp}) there is a good agreement up to a temperature of 550°C after which the theoretical curve begins to grow somewhat faster. During the experimental determination, one should keep in mind the possible change of the sample dimensions and the error during the work with regard to the dilatometrically determined softening temperature of this glass T_{od} = 544°C [19]. By comparing the theoretically obtained curves for the nucleation rate of I_{teo} and the growth of U_{teo} crystals, we can determine that the areas of nucleation and crystal growth of the tested glass partially overlap, ie. the region of simultaneous crystal growth and nucleation occurs after 580°C. Fig. 6, shows the nucleation and growth region of LAGP glass crystals in the temperature range of 500-600°C. From the picture, it can be noticed that the overlap of the area is more significant, ie. simultaneous crystal growth and nucleation occur after 580°C. More intense crystal growth begins after 600°C.

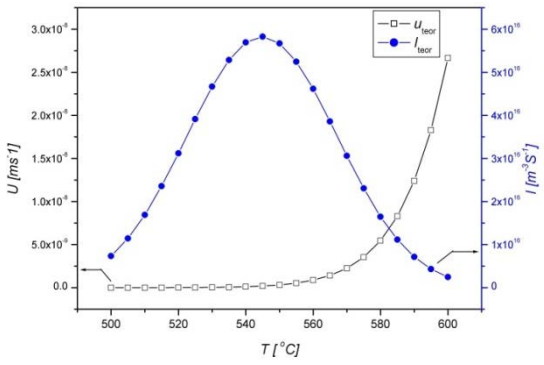

Fig. 6. Comparative presentation of the theoretical crystal growth rate and nucleation of LAGP glass in the temperature range 500-600°C.

This results indicate (Fig. 6) that there is no significant simultaneous nucleation and growth of crystals in the examined area. This effect can be attributed to the addition of alumina to the glass. Accordingly, volume crystallization and separate nucleation and crystal growth process are a significant finding, as it enables controlling the glass ceramic microstructure [17, 19, 21].

The transition time τ (unsteady-steady period, time to establish a stationary rate, τ=48σηλ5*N*a²/πΔG^2, $\sigma_{(T)}$ = – 0.05124 + (1.98958·10^{-4}·*T*), [Jm^{-2}], Δ*G(T)*= - 44.08·(1368.65-*T*)+28.84·[(1368.65-*T*) -*T* ·(ln (1368,65/*T*)], [J/mol]), was calculated by resolving of the Zeldovich-Frenkel equation by Kashchiev and for the examined composition is τ = 134.4 h at T_{Nmax} = 545 °C (I_{max}= 5.83·10^{16} m^{-3}s^{-1}) [12, 19, 22, 23].

Starting from the equation for the crystal growth rate (Eq. 1) and its rearrangement, series development and logarithmization, we arrive at the following expression [24]:

$$\ln\left[\frac{U}{(\Delta T)^2}\right] = \ln K - \frac{\Delta G`_D}{RT} \qquad (4)$$

where the constant $K = \lambda^2\ \Delta H_m^2/(4\pi\sigma V_m h N_A T_m^2)$, $\Delta T = T_m - T$, undercooling interval, T_m - crystal melting temperature; *T*– the temperature at which the dependence is determined.

From Eq. 4, it can be determined the activation energy of crystal growth $\Delta G`_D$ using the values for the crystal growth rate (*U*) and the melting temperature determined by the DSC method (figure not shown) [19]. By representing the relation ln[$U/(\Delta T)^2$] on the ordinate, and 1/*T* on the abscissa from the slope of the obtained rectilinear dependence, $\Delta G`_D$ is determined. Fig. 7, shows the dependence of ln [$U/(\Delta T)^2$] as a function (1/*T*) with the theoretical U_{teo} and experimental U_{exp} values of the crystal growth rate.

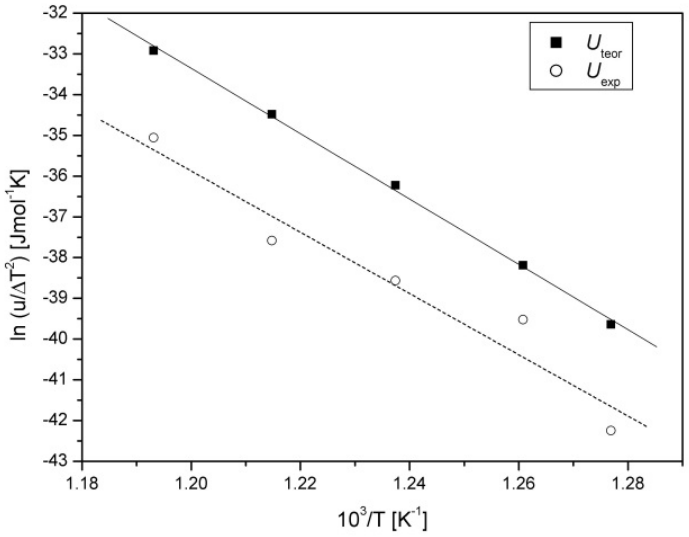

Fig. 7. Dependence of ln [$U/(\Delta T)^2$] as a function of reciprocal temperature (1/*T*) in LAGP glass.

From the slope of the obtained lines, the activation energy of crystal growth in the examined temperature range (500-575°C) was calculated theoretically $\Delta G_{D,\ teo}$ = (665 ± 16) kJ / mol, or experimentally $\Delta G_{D,\ exp}$ = (628 ± 62) kJ / mol. It can be noted that there is a good agreement between the theoretical and experimental values of the growth activation energies of the LAGP glass phase $LiGe_2[PO_4]_3$ crystals.

4. Conclusion

The crystal growth rate of $LiGe_2[PO_4]_3$ phase in the $22.5Li_2O{\cdot}10Al_2O_3{\cdot}30GeO_2{\cdot}37.5P_2O_5$ stoichiometric glass composition was studied. It has been shown that the theoretical temperature dependences of the crystal growth rate tend to an extremum at T_{Gteo}^{max} = 980°C, and the maximum growth rate is $U_{teo}^{max} = 1.35{\cdot}10^{-3}$ ms^{-1}. The experimental growth rates were determined up to T=565°C with a growth rate $U=1.68{\cdot}10^{-11}$ ms^{-1}. The theoretical $\Delta G_{D,\,teo}$ = (665 ± 16) kJ / mol and experimental values $\Delta G_{D,\,teo}$ = (628 ± 62) kJ / mol of the growth activation energies of the LAGP glass phase $LiGe_2[PO_4]_3$ crystals were determined.

Acknowledgments

The authors are grateful to the Ministry of Education, Science and Technological Development of the Republic of Serbia for the financial support (grant contract No.: 451-03-68/2022-14/200023 and 451-03-68/2021-14/200135).

5. References

1. T. Magrinia, F. Bouvilleb, A. R.Studarta, Open Ceramics, 6 (2021) 100109.
2. R. A. A. Wahab, M. H. M. Zaid, K. A. Matori, M. K. Halimah, H. A. A. Sidek, Y. W. Fen, A. Abdu, M. F. M. Shofri, S. H. Jaafar, Sci. Sinter., 54 (2) (2022) 223-233.
3. V. G. Molina, A. P. Parra, P. A. M. Aguilar, R. G. Tapia, M. C. R. González, I. Rosales-Cadena, M. Vlasova, Sci. Sinter., 54 (3) (2022) 249-264.
4. P. Birke, F. Salam, S. Döring, W. Weppner, Solid State Ion., 118 (1999) 149-157.
5. M. Cretin, P. Fabry, J. Eur. Ceram. Soc. 19 (1999) 2931-2940.
6. S.D. Matijašević, M.B. Tošić, J.N. Stojanović, S.R. Grujić, V.D. Živanović, J.D. Nikolić, M.S. Đošić, Ceram-Silikàty, 56 (1) (2012) 61-68.
7. C. Sun, J. Liu, Y. Gong, D. P.Wilkinson, J. Zhang, Nano Energy, 33 (2017) 363-386.
8. W.Vogel,W.Holand, Angew.Chem.Int.Ed.Engl., 26 (1987) 527-544.
9. V. S. Topalović, S. R. Grujić, V. D. Živanović, S. D. Matijašević, J. D. Nikolić, J. N. Stojanović, S. V. Smiljanić, Ceram. Int., 43 (15) (2017) 12061-12069.
10. J. D. Nikolić, S. V. Smiljanjić, S. D. Matijašević, V. D. Živanović, M. B. Tošič, S. R. Grujić, J. N. Stojanović, Process. Appl. Ceram., 7 (4) (2013) 147-151.
11. J. MCGinty, N. Vazdanpanah, C.Price, J. H. Ter Hors, J. Sefcik, The Handbook of Continious Crystallization, Ed. N. Yazdanpanah, Z. Nagy, The Royal Society of Chemistry, London 2020, p.1-50.
12. S. D. Matijašević, S.R. Grujić, J. D. Nikolić, V. S. Topalović, V. V. Savić, S. N. Zildžović, N. J. Labus, Sci. Sinter., 54 (3) (2022) 321-334.
13. G. Sycheva,. J. Cryst. Process Technol., 6 (2016) 29-55.
14. J. Fu, Solid State Ion., 104 (1997) 191-194.
15. N.Anantharamulu, K.K.Rao, G.Rambabu, B.V.Kumar, V.Radha, M.Vithal, J.Mater.Sci., 46 (2011) 2821-2837.
16. P.Maldonado-Manso, E. R. Losilla, M. Martínez-Lara, M. A. G. Aranda, S. Bruque, F. E. Mouahid, M. Zahir, Chem. Mater., 15 (9) (2003) 1879-1885.
17. S. D. Matijašević, S. R. Grujić, V. S. Topalović, J. D. Nikolić, S. V. Smiljanić, N. J. Labus, V. V. Savić, Sci. Sinter., 50 (2) (2018) 193-203.
18. M. F. Barker, Tian-He Wang, P. F. James, Phys. Chem. Glasses, 29 (1988) 240-248.
19. S. D. Matijašević, V. S. Topalović, S. R. Grujić, V. V. Savić, J. D. Nikolić, N. J. Labus, S. N. Zildžović, Sci. Sinter., 53 (3) (2021) 301-310.

20. S. V. Smiljanić, S. R. Grujić, S. D. Matijašević, J. N. Stojanović, J. D. Nikolić, V. V. Savić, D. Z. Popović, J. Therm. Anal. Calorim., 146 (4) (2021) 1569–1576.
21. D. Kosanović, J.Živojinović, J. Vujančević, A. Peleš, V. A. Blagojević, Sci. Sinter., 53 (3) (2021) 285-299.
22. D. Kashchiev, Surface Sci., 14 (1969) 209-220.
23. Clouet, ASM Handbook, Volume 22A: Fundamentals of Modeling for Metals Processing, Ed. D.U. Furrer and S.L. Semiatin, ASM International, Novelty, Ohio, United States 2009, p. 203-219.
24. S. R. Grujić, N. S. Blagojević, M. B. Tošić, V. D. Živanović, Z. S. Aćimović-Pavlović, J. Serb. Chem. Soc., 75 (11) (2010) 1595-1604.

Сажетак: *Проучавана је брзина раста кристала $LiGe_2(PO_4)_3$ из литијум германијум-фосфатног стакла. Стакло је хомогенизовано коришћењем претходно успостављених температурно-временских услова, који омогућавају уклањање испарљивих материја из стакленог растопа. Атомска апсорпциона спектроскопска (ААС) метода је коришћена за одређивање хемијског садржаја добијеног стакла, а скенирајући електронски микроскоп (СЕМ) је коришћен за одређивање изотермног процеса раста кристала. Одређене су експерименталне и теоријске вредности брзине раста кристала.*

Кључне речи*: литијум-германијум-фосфатно стакло, раст кристала, СЕМ.*